



HAL
open science

Design and potentiality of an apparatus for measuring yarn/yarn and fabric/fabric friction

Gilles Hivet, Samir Allaoui, Boun Toum Cam, Pierre Ouagne, Damien Soulat

► **To cite this version:**

Gilles Hivet, Samir Allaoui, Boun Toum Cam, Pierre Ouagne, Damien Soulat. Design and potentiality of an apparatus for measuring yarn/yarn and fabric/fabric friction. *Experimental Mechanics*, 2012, 52 (8), pp.1123-1136. 10.1007/s11340-011-9566-0 . hal-00772343

HAL Id: hal-00772343

<https://hal.science/hal-00772343>

Submitted on 10 Jan 2013

HAL is a multi-disciplinary open access archive for the deposit and dissemination of scientific research documents, whether they are published or not. The documents may come from teaching and research institutions in France or abroad, or from public or private research centers.

L'archive ouverte pluridisciplinaire **HAL**, est destinée au dépôt et à la diffusion de documents scientifiques de niveau recherche, publiés ou non, émanant des établissements d'enseignement et de recherche français ou étrangers, des laboratoires publics ou privés.

Design and potentiality of an apparatus for measuring yarn/yarn and fabric/fabric friction.

G. Hivet, S. Allaoui, B.T. Cam, P. Ouagne, D.Soulat

Laboratoire PRISME, UPRES EA 4229, Université d'Orléans, Polytech'Orléans, 8 rue Léonard de Vinci 45072 Orléans Cedex 2, France

Keywords: RTM, woven reinforcement, friction, fabrics, contact, tribology, textiles, friction measurements.

The market demand for thicker complex shaped structural composite parts is increasing. Processes of the Liquid Composite Moulding (LCM) family, such as Resin Transfer Moulding (RTM) are considered to manufacture such parts. The first stage of the RTM process consists in the preforming of the part. During the pre-forming of multilayered reinforcements, frictions between the plies occur and need to be taken into account for the forming simulation. An experimental device designed to analyse the ply/ply and ply/tool frictions has been set up. The different set up steps of the device are described. First results are presented, which show the ply/ply friction behaviour for a glass plain weave fabric. A specific contact behaviour has been observed for dry reinforcement fabric in comparison to non-technical textiles. A honing effect classically observed in dry fabric testing has also been pointed out through cyclic experiments. It can be attributed to both fibre material abrasion and fibre reorganisation inside the yarn.

1 Introduction

The use of fibre reinforced composites in various industries and especially in the transportation area is increasing because lighter complex shaped parts can be manufactured. Processes of the LCM (Liquid Composite Moulding) family, such as RTM (Resin Transfer Moulding), can be considered to elaborate such parts. The first step of the process consists in draping a dry preform before liquid resin is injected. The preforming stage is a delicate phase. Indeed, the mechanisms involved during this stage are complex, very different from those occurring during the stamping of metallic sheets, and are far from being fully understood [1]. Among the strategies that can be used to optimise LCM processes, finite element forming simulation is one of the most promising. Many methods have been proposed recently to achieve representative sheet forming simulations for

one layer of dry or thermoplastic fabric, through different types of finite elements (trusses, shells, membrane elements), with continuous, discrete or semi-discrete approaches [2-9]. Several key entry parameters for the simulation models need to be determined. The mechanical properties of a fabric ply have been widely studied [10-20], and many teams are still working on this topic to refine the knowledge of the composite community. However, in addition to the ply properties, the fabric/tool contacts and, when dealing with multi-ply forming, the fabric/fabric contact have to be studied and modelled. Concerning composite reinforcements, the tool/fabric contact and, to a lower extent, the yarn/yarn contact have been investigated by different authors, for carbon fibre reinforced thermoplastics or dry fabrics [21-27].

Accurate models of both the ply mechanical properties and the tool/ply contact are crucial when dealing with the forming of one dry ply. However, since composite parts are getting thicker, several layers of fabric are used to manufacture them. Up to now, numerical studies carried out to simulate the multi-layer forming of dry fabrics have used very approximate modelling of the contact between layers. For instance, an approximate friction coefficient, which is independent from the yarns angle, is used by Hamila *et al.* [9]. In addition, preliminary multi-layer forming tests confirmed the significant influence of the relative positioning of the dry plies against one another [28]. This sensitivity of the process to the layer stacking is clearly due to the contact between the layers. It reflects the ability of two layers to glide one on the other during the sheet forming process. It is therefore necessary to better understand the contact behaviour between the sheets of woven reinforcement during that stage, in order to properly understand, optimize and model the first stage of the RTM process.

Different studies concerning the forming of thermoplastic pre-impregnated reinforcements have identified the mechanical phenomena involved during the sliding friction between two fabric plies ([29, 27, 22, 30] for example). They point out the influence of the orientation of the different layers. They also come to the conclusion that this influence could be attributed to the friction variability ([30]). Above all, these papers demonstrate that the friction taking place during the forming of CFRTMP is mainly a viscous friction. Consequently, models based on the fact that the viscous interlayer plays a major role in the inter-ply and tool-ply slip are proposed for the tool/ply or ply/ply friction [3, 31, 32]. However, since the contact behaviour is mainly governed by the resin film leading to a viscous friction,

these results cannot be used to quantify and analyse the friction between dry fabrics. The CF RTP models make it possible to study the influence of the yarns orientation and the contact pressure, but the phenomena involved in dry fabric forming are expected to be different, as the fabric mesostructure should have a much more significant influence on the contact behaviour between dry fabrics. Moreover, the mesoscopic irregularities of the fabric surface combined with the more or less complex weaving may lead to consider models with assumptions and parameters ignored in the classical Coulomb's approach for metallic materials. As a consequence, experiments concerning dry fabric frictions at different scales need to be carried out.

Studies investigating dry fabric frictions can be found in the textile scientific community, [33-42] and are among the most relevant over the past few years. However, the yarns are different from those used in composite reinforcements, in terms of mechanical properties and geometry. Therefore, a direct use of the textile results seems difficult, and a dedicated study concerning composite reinforcement is necessary. The goal of this paper is then to propose an analysis of the contact behaviour between two layers of different dry technical fabrics, using a specific device. This equipment was designed to investigate fabric/metal and yarn/yarn frictions, but the main application should concern the fabric/ fabric dry friction. After a short presentation of the device principles, first results obtained on fabric/fabric contact will be given, demonstrating the potential of the device for the study of fabric/fabric friction.

2 Description of the device

2.1 DEVICE PRINCIPLES

During the forming of multi-ply composite reinforcements, and particularly for curved parts, the dry fabric plies glide on each other, especially when the plies are oriented in different directions. The sliding movement is therefore an important factor to understand, in order to improve the process parameters or simulate it accurately. Since only few studies concerning the friction of composite dry fabrics have been performed, the mechanical phenomena involved during the contact between two layers of fabrics are not really known and understood. It is therefore highly necessary to start with experimental observations. When considering experimental investigations on dry fabric frictions,

various mesoscopic heterogeneities should be considered, due to the interlacement of yarns which width and thickness have a millimeter order of magnitude . In addition, very different unit cell sizes and anisotropy also have to be dealt with. This suggests that specific experimental equipment should be considered to take into account these specifications [10-19].

As mentioned in the introduction, the influence of the relative orientation between the plies implies that the displacement direction according to the yarns orientation should be controlled very accurately . Finally, a simple Coulomb friction coefficient is not expected to take into account the physical phenomena involved. The parameters influencing the friction coefficient should lead to a specific behaviour.

Considering all these constraints, the classical principle consisting in two plane surfaces sliding on each other is considered to be the most promising for this study. This principle has besides been chosen by most of the teams working on fabric friction ([43, 35, 44, 22, 45, 36, 40, 24], for instance). The device proposed here consists in a moving sample (the bottom one) sliding horizontally in a specified direction, at a determinate and adjustable speed, on a fixed top sample (Figure 1). The top sample is fixed and linked to the ground through a load sensor and different joints that will be detailed hereafter. The load sensor measures the tangential loads induced by the contact reaction.

This experimental principle is very simple and directly related to the interply sliding during forming. However, the main difficulty with plane/plane measurements is to ensure a full plane/plane contact with a uniform loading. This point is essential as the mesoscopic heterogeneities are expected to be very sensitive to this defect and the measured values may be consequently affected. Different strategies can be considered to get a uniform pressure distribution. Applying a resultant load (through a cylinder for instance) on one or both samples (through its support) could be efficient but would impose either a complex and expensive design or an expensive precise manufacturing [22].

Furthermore, these techniques are all the less indicated for our application that a finite vertical movement of the sample due to the mesoscopic heterogeneity of the weaving will probably be observed during the tests. Among the existing solutions, the use of gravity seems to be the simplest because a constant pressure distribution on the whole area of the sample can be obtained through a clever mass distribution of the unit (support + sample), and an horizontal positioning of the two units is

relatively easy to realise. However, since dynamic measurements are considered, it is necessary to apply a constant accurate load, and a specific procedure is proposed in the following section.

The kinematical scheme of the retained solution is presented in Figure 2. The bottom sample is rigidly and accurately guided by a linear system in order to translate horizontally in a fixed direction.

The upper steel plate, supporting the tested sample, is linked to the load sensor using two classical balls joints, so that the sample remains in a plane positioning and transmits nothing but the longitudinal load to be measured (Figure 2Figure 17). Furthermore, the sensor is consequently protected against accidental torques.

The lateral positioning of the upper sample is ensured by a linear joint. The linear joint (Figure 2Figure 17) is obtained with two rollers rolling on two vertical plates. The functional play in this connection enables a little rotation around axis x in order to respect the preponderant plane positioning. Indeed, the top sample (i.e. support + sample) lays freely upon the horizontal bottom sample. The sample is only guided laterally in the horizontal direction, in order to ensure that a plane contact is respected.

2.2 PRESSURE DISTRIBUTION DURING MEASUREMENTS

2.2.1 PROBLEM AND PROPOSED SOLUTION

The previously exposed principle theoretically makes it possible to obtain a static equi-distribution of the pressure, but it has to remain so during measurements. Locally, an equi-distribution of the pressure is much more difficult to achieve, because of all the mechanical phenomena involved.

Several assumptions need to be taken into account:

- the lower plane is perfectly horizontal, the tangential loads and displacement take place along direction x .
- inertia effects are neglected since a constant speed is used during the measurements
- If C is the centre of the contact surface, R one possible centre of the joint local coordinate system of the linear joint, G the centre of mass of the upper sample unit and S is the centre of the ball joint (Figure 3), the loads exerted on the top sample can be modelled as follows:

- Contact with the bottom sample: $T_{contact} = \{N_c \vec{y} + T_c \vec{x} | \vec{M}_c\}_C^{R(x,y,z)}$, N_c is the normal load, T_c the tangential (friction) load and M_c is the torque due to the possible non uniform pressure distribution (Figure 3). (1)

- Load exerted by the load sensor $T_{sensor/sample} = \{T_{ss} \vec{x} | \vec{0}\}_S^{R(x,y,z)}$ with $\vec{CS} = x_S \vec{x} + y_S \vec{y}$ (2)

- Load exerted by the linear joint (to avoid any spurious z displacement)

$$T_{bearing/sample} = \{Z_B \vec{z} | M_B \vec{x}\}_R^{R(x,y,z)} \text{ with } \vec{CR} = x_R \vec{x} + y_R \vec{y} + z_R \vec{z} \quad (3)$$

- Weight of the unit support + sample: $T_{weight} = \{-mg \vec{y} | \vec{0}\}_G^{R(x,y,z)}$ with $\vec{CG} = x_G \vec{x} + y_G \vec{y}$ (4)

The moment balancing along direction x at point C (Figure 3) can then be written as follows:

$$M_C - T_{ss} y_S - mg x_G = 0 \quad (5)$$

If the centre of mass is supposed to be at the vertical of the centre of the contact surface C, then we obtain:

$$M_C - T_{ss} y_S = 0 \quad (6)$$

During sliding, tangential loads appear therefore (Figure 3):

$$T_{ss} = -T_c \neq 0 \quad (7)$$

If $y_S \neq 0$ the contact torque at the centre C of the contact area cannot be neglected. The load distribution is consequently no more homogeneous. In order to avoid this unwished torque, $y_S = 0$ could be imposed, i.e. S has to be located in the contact plane. But since fabric thicknesses vary in a wide range depending on the yarn and the weaving type (from thin 2D fabrics to thick interlocks or 3D fabrics), the height of the S point should be adjusted for each type of studied material. Another approach consists in reducing the discrepancy induced by this phenomenon until it becomes negligible with respect to the accuracy the user is looking for. Indeed, this spurious torque can be balanced by a slight displacement of the centre of mass. The centre of mass displacement can be expressed using the coordinate x_G of the real centre of mass. In order to obtain $M_C = 0$, back to equation (5) written in the case $x_G \neq 0$, the centre of gravity has to be located at the abscissa x_G with

$$x_G = -\frac{T_{ss} y_S}{mg} \quad (8)$$

A correct positioning of the centre of gravity of the upper sled can theoretically enable a correct equilibrium distribution of the pressure. Nevertheless, the real time positioning of this centre of gravity is not

possible. Therefore, in order to control the variations involved during the test (variations in the friction coefficient, in the sample altitude,...), the sensitivity of the pressure repartition to parameter variations (x_G, T_{ss}, y_s) shall be studied. An experimental validation is also conducted to confirm the stability of the test.

2.2.2 THEORETICAL EVALUATION OF THE DISPERSIONS OBTAINED

The pressure repartition defect is expressed using Equation 13:

$$d = \frac{p_{Max} - p_{Min}}{p_{avg}} \quad (9)$$

In which p_{avg} is the average value of p on the contact surface.

The contact surface is defined by the dimensions of the top sample (a rectangle in the (x,z) plane with $l_s = 80mm$ and $L_s = 100mm$ (Figure 3Figure 18). Due to the symmetry of the device, the pressure distribution heterogeneity is assumed to only take place in direction x and to induce a linear variation of the pressure along the x coordinate, so that the pressure on the contact surface can be written:

$$p(x, z) = p(x) = p_0 + kx \quad (10)$$

The balance equations can be written as follows:

$$N_c = \int_{-l_s/2}^{l_s/2} \int_{L_s/2}^{L_s/2} p(x) dx dz = mg \quad (11)$$

$$\Rightarrow N_c = \int_{-l_s/2}^{l_s/2} \int_{L_s/2}^{L_s/2} p_0 + kx dx dz = mg \quad (12)$$

$$\Rightarrow p_0 = p_{avg} = \frac{mg}{L_s l_s} \quad (13)$$

The spurious torque induced by the pressure variation can be expressed according to the following equations:

$$M_c = \int_{-l_s/2}^{l_s/2} \int_{-L_s/2}^{L_s/2} \vec{CM} \wedge (p_0 + kx) \vec{y} dx dz = T_{ss} y_s + mg x_G \quad (14)$$

$$M_c = \frac{k l_s L_s^3}{12} = T_{ss} y_s + mg x_G \quad (15)$$

$$\Rightarrow k = 12 \frac{T_{ss}y_s + mgx_G}{l_s L_s^3} \quad (16)$$

As a consequence, the pressure repartition can be given by:

$$p(x, z) = p(x) = \frac{mg}{L_s l_s} + 12 \frac{T_{ss}y_s + mgx_G}{l_s L_s^3} x \quad (17)$$

$$d = \frac{12 \frac{T_{ss}y_s + mgx_G}{l_s L_s^3} L_s}{\frac{mg}{L_s l_s}} \quad (18)$$

All test parameters being fixed, a coefficient μ can be introduced.

$$\mu = \frac{T_{ss}}{mg} \quad (19)$$

So the pressure repartition defect is expressed using Equation 24:

$$d = 12 \frac{\mu y_s + x_G}{L_s} \quad (20)$$

The acceptable value admitted for d in this work for such type of measurement in the field of dry fabrics is $\pm 5\%$. A better accuracy cannot reasonably be expected, considering the dispersions between the different unit cells of the same fabric. Thus the following relationship is obtained:

$$\frac{L_s}{240} \sim 0.42 > \mu y_s + x_G > -\frac{L_s}{240} \sim -0.42 \quad (21)$$

In order to stay within the 10% deviation of the pressure dispersion, relation (25) has to be validated.

As an example, assuming a careful positioning of the centre of gravity at the initial state, this defect can be majored by 0.2 mm and a maximum variation of μ between 0 and 1 can be observed. The acceptable deviation for y_s is really reasonable

$$-0.32 < y_s < 0.32 \quad (22)$$

As a conclusion, the proposed design is capable of responding to the pressure repartition needed.

With a good estimation of the average friction coefficient and the average y position of the contact surface (obtained with a first test for instance), the centre of mass can be placed accurately enough.

This has been verified by a sensitivity study on metallic, polymers and woven materials.

2.3 TECHNOLOGICAL OVERVIEW

The device designed according to the principles detailed in the previous sections is presented on Figure 4. The bottom sample (Figure 5) is clamped by screws on a PVC plate on a 60 cm long and 9 cm wide steel plate (Figure 6). The sample is manually tensed a little so that it does not wrinkle; the amount of tension introduced is therefore low enough to be neglected, especially when considering the high amount of tension that can be undergone by dry fabrics.

A brushless motor and an electronic speed controller linked via an Oldham joint to a ball screw/bold system (Figure 6) is used to imposed the displacement of the steel plate. This enables to obtain a speed variation from 0 to 100 mm/s with a 50 cm displacement range. These values have been chosen in reference to the classical speed values used for the measurement of friction coefficients in both textiles and composite materials. This speed range also matches the velocities involved during the composite forming processes.

The velocity ramp is piloted to avoid dynamic effects, especially at high speed ranges. The velocity profile can be adjusted depending on the required steady state velocity. The velocity profile theoretically obtained is governed by equation (1).

$$v(t) = v_{Max} \left(1 - e^{-t/\tau} \right) \quad (23)$$

The top sample (Figure 7) is clamped on a 10 cm long and 8 cm wide steel plate. The tangential load is measured through an FGP FN3148 50 N capacity sensor. It is calibrated and used in the 0-20N range in order to get a fully acceptable 0.01N accuracy.

A rubber damper and a low pass filter (25Hz to 100Hz) chosen in match with the natural frequencies of the different elements limit the vibrations and enable a smoother signal without interfering with the steady state measurement. A Burster Digiforce acquisition system is used to record up to 4000 measurements at a frequency of up to 5000 Hz, which is convenient for our application.

2.4 DEVICE VALIDATION

The device has been validated on a steel/steel friction at different speeds (0.5, 1.5, 6 cm/sec) and normal loads (7.4, 17.2 and 24.5 N). The steel considered is C48 with no resurfacing and lubrication. The average steady state coefficient of friction (that is targeted by this study) obtained with these tests is about 0.190 ± 0.008 , which is in good correlation with results found in the literature and has a good repeatability ($\pm 5\%$) in the range of what was expected.

3 Dry fabric/Dry fabric friction

3.1 MATERIALS TESTED

Three different woven fabrics with different architectures have been used for this first experimental study (Figure 8): two glass plain weave fabrics and a carbon twill weave. The first glass plain weave is a 0.6 mm thick Tissa+ glass plain weave. The yarns have a width of 1.1 mm and an average spacing of 2.3 mm between each other. The second material tested in this work is a 0.75 mm thick “balanced” glass plain weave, with 3.7 mm wide yarns and a 5 mm average spacing between weft yarns and 4.5 mm spacing between warp yarns. The carbon twill weave is the Hexcel G986. It has an areal weight of 285g/m^2 and is constituted of HTA 5131 6K yarns. The Average yarn width is 1.68 mm (~ 1.6 mm for warp, ~ 1.8 mm for weft). The average yarns spacing is 2.92 mm (~ 2.91 mm for warp, ~ 2.93 for weft).

3.2 PRELIMINARY RESULTS ON ONE COUPLE OF PLAIN WEAVE SAMPLES

3.2.1 FRICTION LOADS AND COULOMB FRICTION COEFFICIENT

After preliminary tests, a 5 mm/s displacement speed is chosen for the bottom sample. A 15 ms acquisition period is considered to distinguish the frequencies of the different physical phenomena taking place during the measurement. One couple of samples of the first glass plain weave has been submitted to a 10 cycle test with a 0.7 s tempo and a normal force of 10N. The acquisition of 4000 points leads to a test duration of 60s and 30cm gliding between the two samples. Figure 9 shows the results obtained.

As expected, the tangential load, measured when the steady state is reached, is far from being

constant. This conclusion is relatively similar to what has been observed in the different publications cited in the previous sections concerning textiles. Nevertheless, the magnitude of the variations is much higher. The tangential load varies from 2 to 6 N with an average value of about 3.8 N, and a variation with respect to the average value greater than 50%. Consequently, the difference between the responses obtained for composite, thermoplastic materials, garment textiles and technical dry fabrics appears to be significant.

A more accurate analysis of the response enables us to distinguish three characteristic pseudo periods. The first one depicts the undulation of the local maximum values (Figure 9.b). Even if its value is not so easy to quantify, this first period can be approximately evaluated and is equal to about $T_1=60s$. Local minimum values are not submitted to the same type of undulation as the maximum values, and their magnitude is much smaller. A representative period does not appear so clearly, the lack of symmetry is noticeable. The second period is associated to the interval between two maximum load values when the response magnitude is the highest (~6N, Figure 9Figure 24.a, Figure 9Figure 24.d). Its value is about $T_2=1s$. The third one is the duration separating two maximum load values when the response magnitude is the lowest (~4N, Figure 9Figure 24.a, Figure 9.c). Its value is about $T_3=0.5s$. Figure 9.e, depicts the transition between zone A and B.

This preliminary analysis of the first results directly issued from the device reveals a very specific fabric/fabric contact behaviour. The nature of the signals, the amount and the frequencies of the variations are very different from those obtained through tests on metallic, thermoplastic or textile fabrics.

Coulomb's theory is undoubtedly not the best to depict fabric/fabric friction. For complex surfaces such as dry fabrics, the contact behaviour cannot be brought back to a simple variation of a friction coefficient. As will be shown in the next sections, different physical phenomena may occur that are not directly linked to what is classically associated with the friction coefficient. However, a "pseudo" friction coefficient $\mu(t)$ can be introduced according to Coulomb's model, in order to make the results independent from the normal load and to compare the different materials studied in this work. To our knowledge, all the macro-scale forming simulations on dry fabrics consider up to now a single average friction coefficient. It is then interesting to get this average coefficient from our own results, even if we

intend to show that it is far from being enough to correctly represent the complexity of the contact behaviour between dry fabrics.

$$\mu(t) = \frac{T(t)}{N} \quad (24)$$

$$\mu = \frac{1}{\Delta t} \int \frac{T(t)}{N} dt \quad (25)$$

Results will often be expressed giving this friction coefficient, as the friction coefficient follows the same variations as the tangential load (Figure 10).

3.2.2 CYCLING

Cycling results are presented on Figure 11 for this first couple of samples. A grinding effect is observed: the average friction load and standard deviation tend to decrease and then converge toward an asymptotic value. This effect can be attributed to the abrasion of the material itself but also to fibre reorganisations under contact loads. This phenomenon is not surprising because it is classically encountered in dry reinforcements fabric testing, whatever the type of solicitation applied (shear, biaxial, bending,...). Consequently, the number of cycles has to be taken into consideration when looking at the friction results. Two particular values are more interesting: the first cycle and the asymptotic ones. The first because it is the one that is mainly encountered in the multi-layer forming process and the asymptotic value because it makes it possible to perform many tests without replacing the samples.

The influence of the number of cycles is confirmed by the results obtained for the carbon twill weave fabric (Figure 12Figure 27.c,d) and for the second glass plain weave (Figure 12Figure 27.a,b). The higher amount of discrepancies observed for the latest material is due to the weak cohesion of the fibres inside the yarns and to the weak cohesion of the yarns within the fabric. Nevertheless, the average friction coefficient and standard deviation values are as expected decreasing as a function of the increase in the number of cycles.

3.2.3 REPEATABILITY

Other couples of samples of the same Tissa+ glass plain weave fabric have been tested in the same conditions in order to investigate repeatability. The results for two of them are presented on Figure 13a. is representative of what was observed for most of the couples of samples. A comparison with

the results of the preliminary test on Figure 9 indicates that frequencies and magnitudes previously observed in detail A and detail B (Figure 9) are consistent. However, the time-tagged of each of them corresponding to the previously identified period T1 can be significantly different. Figure 13.b shows the extreme case for which only the highest frequency response is observed. The value of period T3 is consistent with the ones obtained for the two other samples but periods T1 and T2 are different from the corresponding periods identified on all the other couples of samples. Because this phenomenon did not appear during the cycling tests it is supposed that this observation is due to the samples positioning in direct relationship with the meso architecture.

3.3 ANALYSIS OF PRELIMINARY RESULTS

At a 0.5 cm/S speed, the two main periods measured in section 3.2.1 respectively represent 2.5mm and 5mm, i.e. values very close to the yarn spacing and twice as big as the yarn spacing. This relation is confirmed by the results of the second glass plain weave and will be investigated further through experiments on other weavings as part of further research. Figure 14 presents an example of results obtained for the second Glass plain weave. They confirm the contact behaviour obtained and the consistency between the period values and the geometrical parameters (weft yarns spacing: 5mm). Average signal periods expressed in millimeters: $T_3 = 5mm$ and $T_2 = 10mm$.

The periods found in the friction response therefore seem to be associated to the meso geometrical parameters of the fabric. This influence can easily be explained through a simple geometrical analysis illustrated on Figure 15.

If the two samples are perfectly superimposed, the highest zone of the bottom layer encounters the lower zone of the upper sample. The contact consists in the superposition of yarn/yarn sliding friction and shocks between the transverse yarns of each sample at the same time everywhere on the sample width (Figure 15), at each period of the unit cell. Consequently, high maximum friction value and variations are observed. This phenomenon is representative of zone B on Figure 9 and Figure 14. This perfectly explains why the non-technical fabrics with lower crimp and thinner yarns are submitted to lower magnitude variations. Shocks are indeed all the more significant that the crimp is high and the yarns are thick.

On the contrary, if the samples are shifted of half a geometrical period (Figure 15), the highest zone of

the bottom layer never impacts the lowest zone of the top layer. This time, the configuration is repeated every half geometrical period and the impact is lower. This therefore leads to lower maximum friction values, lower variations and a signal period value of half the geometrical one. This corresponds to zone A on Figure 9 and Figure 14. Between the two extreme shifts, the signal is a combination of these two contact morphologies, depending on the actual shift between the two samples.

The results obtained on Figure 9 and Figure 14 are therefore due to the modification of the relative displacement between the two samples along the stroke. This displacement is the consequence of the play in the linear joint (between the two plates and the roller), to ensure the preponderant plane positioning between the two samples, and of the difficulty to perfectly align all the yarns of two samples of dry fabrics. Thus, depending on the initial positioning of each sample (shift, angle), there can be more or less relative displacement between the two samples at different location along the samples. Since these first tests, the play has been a little bit reduced so that this phenomenon is reduced.

4 Conclusion

A specific device has been developed to characterise the contact behaviour between two layers of woven fabrics. The knowledge of the contact behaviour between layers of woven fabrics is of particular importance when multiply forming is concerned. The device appeared to be well adapted to investigate fabric friction. Preliminary results have been presented. A honing effect classically observed in dry fabric testing has also been pointed out through cyclic experiments. It can be attributed to both fibre material abrasion and fibre reorganisation inside the yarns.

As expected, a specific contact behaviour is observed for dry reinforcement fabrics in comparison to non-technical textiles (garments,...), yarn/yarn or fabric/metal friction. Particularly, the variations of the contact tangential loads can be very substantial, all test parameters remaining constant. The large amplitude of friction can undoubtedly be explained by the meso architecture of dry fabrics, and especially by the contact between the parallel yarns of the two samples. An intensive analysis with higher sampling frequencies and more complex weavings (interlocks,...) is in progress, in order to help analyse this phenomenon more accurately.

Consequently, using an average friction coefficient will lead to a high amount of uncertainties in the mechanical analysis of these materials. Particularly, the variations of the friction load magnitude

should be considered when trying to optimise multiply forming. The evolution of the relative orientation of the yarns of each ply may result in high variations of the tangential friction forces. This can also lead to manufacturing defaults, such as unweaving or wrinkles. Up to now, finite element codes predicting the forming behaviour of woven reinforcement fabrics do not take into account the evolution of this friction coefficient to accurately model the process. This point should therefore be addressed in future works on this topic with the view of optimising the multiply forming of complex shaped composite parts. Some interesting conclusions have already been obtained, but this device will furthermore make it possible to perform an extensive experimental campaign, so the fabric/fabric contact behaviour can be fully understood and modelled.

- [1] Soulat D. Wendling A. Chatel S. Hivet G., Allaoui S. Analysis of woven reinforcement preforming using an experimental approach. In *ICCM-17, 17th International Conference on Composite Materials.*, Edinburgh International Convention Centre (EICC), Edinburgh, UK, 27 Jul-31 Jul 2009.
- [2] A.K. Pickett, T. Queckbörner, P. De Luca, and E. Haug. An explicit finite element solution for the forming prediction of continuous fibre-reinforced thermoplastic sheets. *Composites Manufacturing*, 6(3-4):237–243, 1995.
- [3] K. Vanclooster, S. Lomov, and I. Verpoest. Simulation of multi-layered composites forming. *International Journal of Material Forming*, 3:695–698, 2010. 10.1007/s12289-010-0865-2.
- [4] R.H.W. ten Thije, R. Akkerman, and J. Huétink. Large deformation simulation of anisotropic material using an updated lagrangian finite element method. *Computer Methods in Applied Mechanics and Engineering*, 196(33-34):3141–3150, July 2007.
- [5] X.Q. Peng and J. Cao. A continuum mechanics-based non-orthogonal constitutive model for woven composite fabrics. *Composites Part A: Applied Science and Manufacturing*, 36(6):859–874, June 2005.
- [6] B. Ben Boubaker, B. Haussy, and J.F. Ganghoffer. Discrete models of woven structures. macroscopic approach. *Composites Part B: Engineering*, 38(4):498 – 505, 2007.
- [7] David Jauffres, James Sherwood, Corey Morris, and Julie Chen. Discrete mesoscopic modeling for the simulation of woven-fabric reinforcement forming. *International Journal of Material Forming*, 3:1205–1216, 2010. 10.1007/s12289-009-0646-y.
- [8] G. Creech and A. Pickett. Meso-modelling of non-crimp fabric composites for coupled drape and failure analysis. *Journal of Materials Science*, 41:6725–6736, 2006. 10.1007/s10853-006-0213-6.
- [9] Nahiene Hamila and Philippe Boisse. A meso macro three node finite element for draping of textile composite preforms. *Applied Composite Materials*, 14:235–250, 2007. 10.1007/s10443-007-9043-1.
- [10] S.V. Lomov and I. Verpoest. Model of shear of woven fabric and parametric description of shear resistance of glass woven reinforcements. *Composites Science and Technology*, 66(7-8):919–933, June 2006.
- [11] J. Launay, G. Hivet, A.V. Duong, and P. Boisse. Experimental analysis of the influence of tensions on in plane shear behaviour of woven composite reinforcements. *Composites Science and*

Technology, 68(2):506–515, February 2008.

- [12] P. Boisse, A. Gasser, and G. Hivet. Analyses of fabric tensile behaviour: determination of the biaxial tension-strain surfaces and their use in forming simulations. *Composites Part A: Applied Science and Manufacturing*, 32(10):1395–1414, October 2001.
- [13] E. de Bilbao, G. Soulat, D. Launay, J. Hivet, and A. Gasser. Experimental study of bending behaviour of reinforcements. *Experimental Mechanics*, 50(3):333–351, 2010.
- [14] J. Cao, R. Akkerman, P. Boisse, J. Chen, H.S. Cheng, E.F. de Graaf, J.L. Gorczyca, P. Harrison, G. Hivet, J. Launay, W. Lee, L. Liu, S.V. Lomov, A. Long, E. de Luycker, F. Morestin, J. Padvoiskis, X.Q. Peng, J. Sherwood, Tz. Stoilova, X.M. Tao, I. Verpoest, A. Willems, J. Wiggers, T.X. Yu, and B. Zhu. Characterization of mechanical behavior of woven fabrics: Experimental methods and benchmark results. *Composites Part A: Applied Science and Manufacturing*, 39(6):1037–1053, June 2008.
- [15] A. Willems, S.V. Lomov, I. Verpoest, and D. Vandepitte. Optical strain fields in shear and tensile testing of textile reinforcements. *Composites Science and Technology*, 68:807–819, 2008.
- [16] T. M. McBride and Julie Chen. Unit-cell geometry in plain-weave fabrics during shear deformations. *Composites Science and Technology*, 57(3):345–351, 1997.
- [17] J. Wang, J. R. Page, and R. Paton. Experimental investigation of the draping properties of reinforcement fabrics. *Composites Science and Technology*, 58(2):229 – 237, 1998. Australasian Special Issue on Manufacturing Processes and Mechanical Properties Characterisation of Advanced Composites.
- [18] Wiggers J. Harrison, P. and A.C. Long. Normalisation of shear test data for rate-independent compressible fabrics. *Journal of Composite Materials*, 42(22):2315–2343, 2008.
- [19] Gilbert Lebrun, Martin N. Bureau, and Johanne Denault. Evaluation of bias-extension and picture-frame test methods for the measurement of intraply shear properties of pp/glass commingled fabrics. *Composite Structures*, 61(4):341–352, September 2003.
- [20] P. Badel, E. Vidal-Sallé, and P. Boisse. Computational determination of in-plane shear mechanical behaviour of textile composite reinforcements. *Computational Materials Science*, 40(4):439–448, October 2007.
- [21] Bilel Ben Boubaker, Bernard Haussy, and Jean-François Ganghoffer. Discrete woven structure model: yarn-on-yarn friction. *Comptes Rendus Mécanique*, 335(3):150 – 158, 2007.

- [22] R. H. W. ten Thije and R. Akkerman. Design of an experimental setup to measure tool-ply and ply-ply friction in thermoplastic laminates. *International Journal of Material Forming*, 2:197–200, 2009.
- [23] S. Rebouillat. Tribological properties of woven para-aramid fabrics and their constituent yarns. *Journal of Materials Science*, 33:3293–3301, 1998. 10.1023/A:1013225027778.
- [24] Jennifer L. Gorczyca, James A. Sherwood, Lu Liu, and Julie Chen. Modeling of friction and shear in thermostamping of composites - part i. *Journal of Composite Materials*, 38(21):1911–1929, 2004.
- [25] Lu Liu, Julie Chen, Jennifer L. Gorczyca, and James A. Sherwood. Modeling of friction and shear in thermostamping of composites - part ii. *Journal of Composite Materials*, 38(21):1931–1947, 2004.
- [26] Ben Nadler and David J. Steigmann. A model for frictional slip in woven fabrics. *Comptes Rendus Mecanique*, 331(12):797 – 804, 2003.
- [27] Gilbert Lebrun, Martin N. Bureau, and Johanne Denault. Thermoforming-stamping of continuous glass fiber/polypropylene composites: Interlaminar and tool laminate shear properties. *Journal of Thermoplastic Composite Materials*, 17(2):137–165, 2004.
- [28] A. Wendling D. Soulat S. Chatel S. Allaoui, G. Hivet. Experimental approach for optimizing dry fabric formability. In *14th European Conference on Composite Materials, Budapest, Hungary, 7-10 june 2010*.
- [29] Mallon PJ. Murtagh AM, Monaghan MR. Investigation of the interply slip process in continuous fibre thermoplastic composites. In *Proceedings of ICCM-9, Madrid, Spain*, page 311–318., 1994.
- [30] K. Vanclooster, S. Van Goidsenhoven, S. Lomov, and I. Verpoest. Optimizing the deepdrawing of multilayered woven fabric composites. *International Journal of Material Forming*, 2:153–156, 2009. 10.1007/s12289-009-0522-9.
- [31] R. ten Thije, R. Akkerman, L. van der Meer, and M. Ubbink. Tool-ply friction in thermoplastic composite forming. *International Journal of Material Forming*, 1:953–956, 2008. 10.1007/s12289-008-0215-9.
- [32] Jennifer L. Gorczyca-Cole, James A. Sherwood, and Julie Chen. A friction model for thermostamping commingled glass-polypropylene woven fabrics. *Composites Part A: Applied Science and Manufacturing*, 38(2):393 – 406, 2007.
- [33] J. O. Ajayi, H. M. Elder, E. G. Kolawole, K. A. Bello, and M. U. Darma. Resolution of the stick-

slip friction traces of fabrics. *Journal of the Textile Institute*, 86(4):600–609, 1995.

[34] J. O. Ajayi and H. M. Elder. Fabric friction, handle, and compression. *Journal of the Textile Institute*, 88(3):232–241, 1997.

[35] A. A. A. Jeddi, S. Shams, H. Nosraty, and A. Sarsharzadeh. Relations between fabric structure and friction: Part i: Woven fabrics. *Journal of the Textile Institute*, 94(3):223–234, 2003.

[36] P. M. Taylor and D. M. Pollet. The low-force frictional characteristics of fabrics against engineering surfaces. *Journal of the Textile Institute*, 91(1):1–15, 2000.

[37] J. P. P. Marcicano, C. C. Tu, and H. G. Rylander. Measurement of the transverse yarn-on-solid coefficient of friction. *Journal of the Textile Institute*, 95(1):349–357, 2004.

[38] USA B S Gupta, NCSU, editor. *Friction in textile materials*. Woodhead Publishing Limited, 2008.

[39] Bhupender S. Gupta and Yehia E. El Mogahzy. Friction in fibrous materials part i: Structural model. *Textile Research Journal*, 61(9):547–555, 1991.

[40] Luis Virto and Arun Naik. Frictional behavior of textile fabrics : Part ii dynamic response for sliding friction. *Textile Research Journal*, 70(3):256–260, 2000.

[41] Mario Lima, Rosa M. Vasconcelos, Luis F Silva, and Joana Cunha. Fabrics made from non-conventional blends: What can we expect from them related to frictional properties? *Textile Research Journal*, 79(4):337–342, 2009.

[42] A.D. Vickers, D.G. Beale, Y.T. Wang, and S. Adanur. Analyzing yarn-to-surface friction with data acquisition and digital imaging techniques. *Textile Research Journal*, 70(1):36–43, 2000.

[43] Adrian M. Murtagh, John J. Lennon, and Patrick J. Mallon. Surface friction effects related to pressforming of continuous fibre thermoplastic composites. *Composites Manufacturing*, 6(3-4):169 – 175, 1995. 3rd International Conference on Flow Processes in Composite Materials 94.

[44] O.J Ajayi. Fabric smoothness, friction, and handle. *Textile research journal*, 62(1):52–59, 1992.

[45] K. Vanclooster, S. Lomov, and I. Verpoest. Investigation of interply shear in composite forming. *International Journal of Material Forming*, 1:957–960, 2008. 10.1007/s12289-008-0216-8.

Figures:

Figure 1: Scheme of the device

Figure 2 : Kinematical scheme of the device (Top view)

Figure 3 : Geometrical parameters and points location

Figure 4 : External view of the friction device

Figure 5 : Top and Bottom glass plain weave sample

Figure 6 : External view of the bottom unit

Figure 7 : External view of the top unit of the device

Figure 8 : Fabrics used for fabric/fabric friction

Figure 9 : Experimental results for the Glass plain weave 1, $v=0.5\text{cm/s}$, $N=10\text{N}$

Figure 10 : Experimental time depending on average friction coefficient for the Glass plain weave 1, $v=0.5\text{cm/s}$, $N=10\text{N}$.

Figure 11 : Average friction coefficient and standard deviation as a function of the number of cycles for a couple of the first glass plain weave samples, $v=5\text{mm/s}$, $N=10\text{N}$.

Figure 12 : Average friction coefficient in function of the number of cycle for the 2nd glass plain weave (a., b.) and the carbon twill weave (c.,d.) .

Figure 13 : Friction coefficient results for another 2 samples identical to glass plain weave 1.

Figure 14 : Results for a couple of samples of the second glass plain weave, a. tangential force response, b., c. Periods in length units for zone A and B.

Figure 15 : Samples relative lateral positioning

Figures :

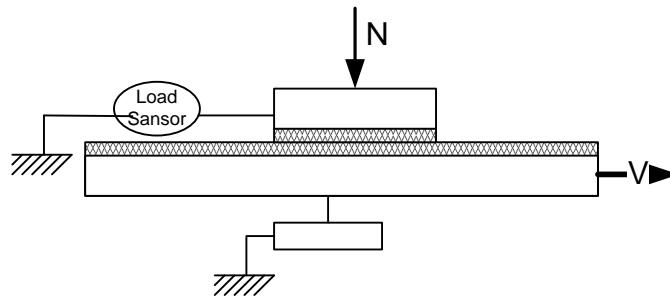


Figure 16 Scheme of the device

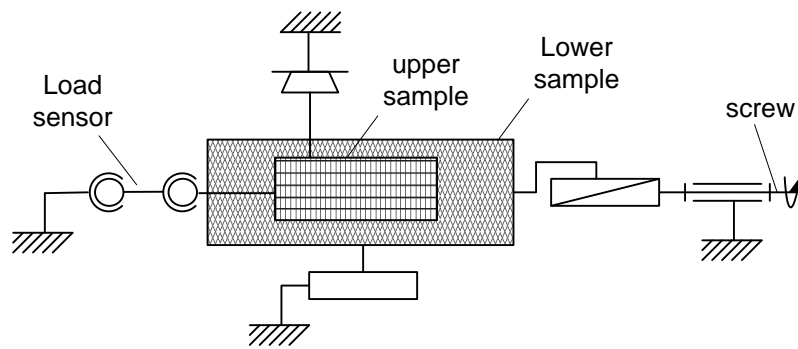


Figure 17 : kinematical scheme of the device (Top view).

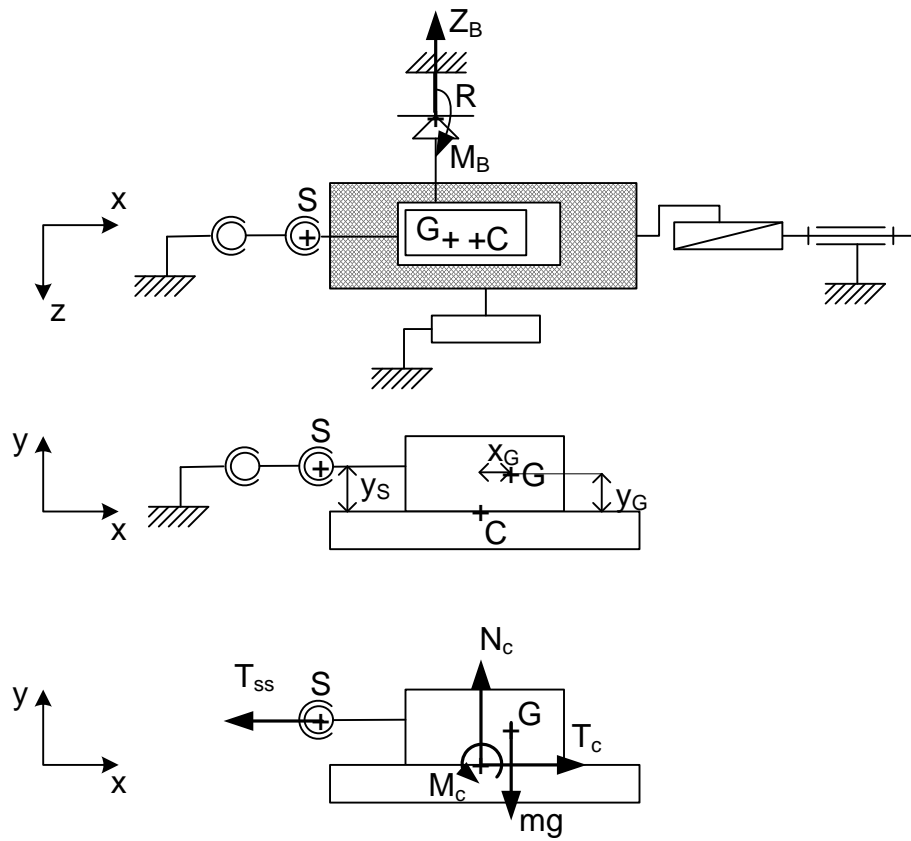


Figure 18 : Geometrical, force parameters and points location



Figure 19 : External view of the friction device.

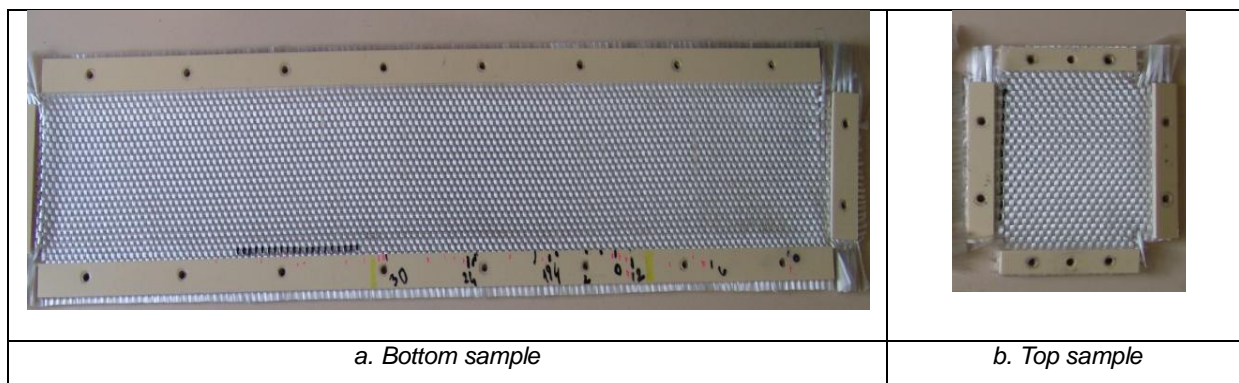


Figure 20 : Top and Bottom glass plain weave sample

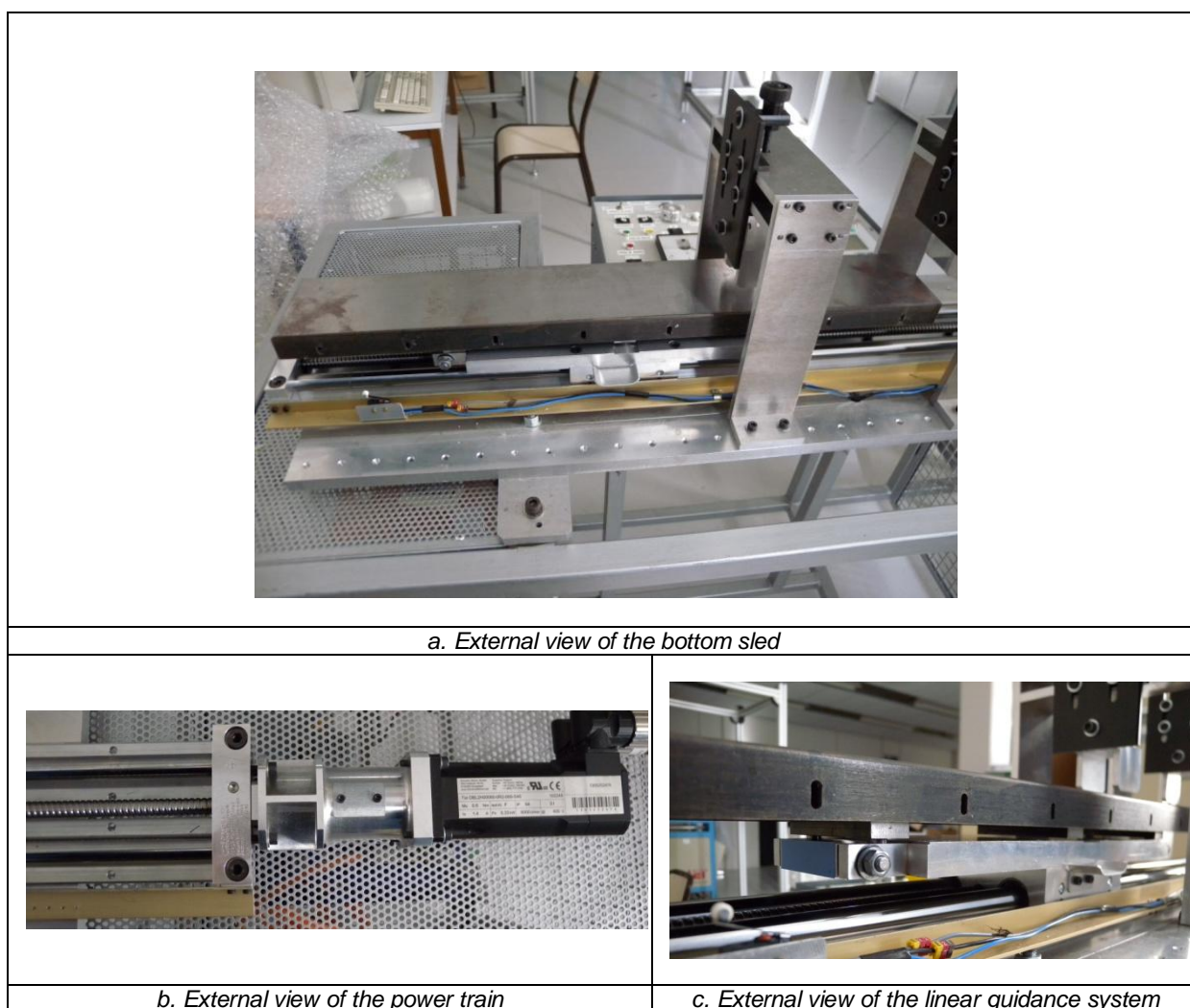


Figure 21 : external view of the bottom unit

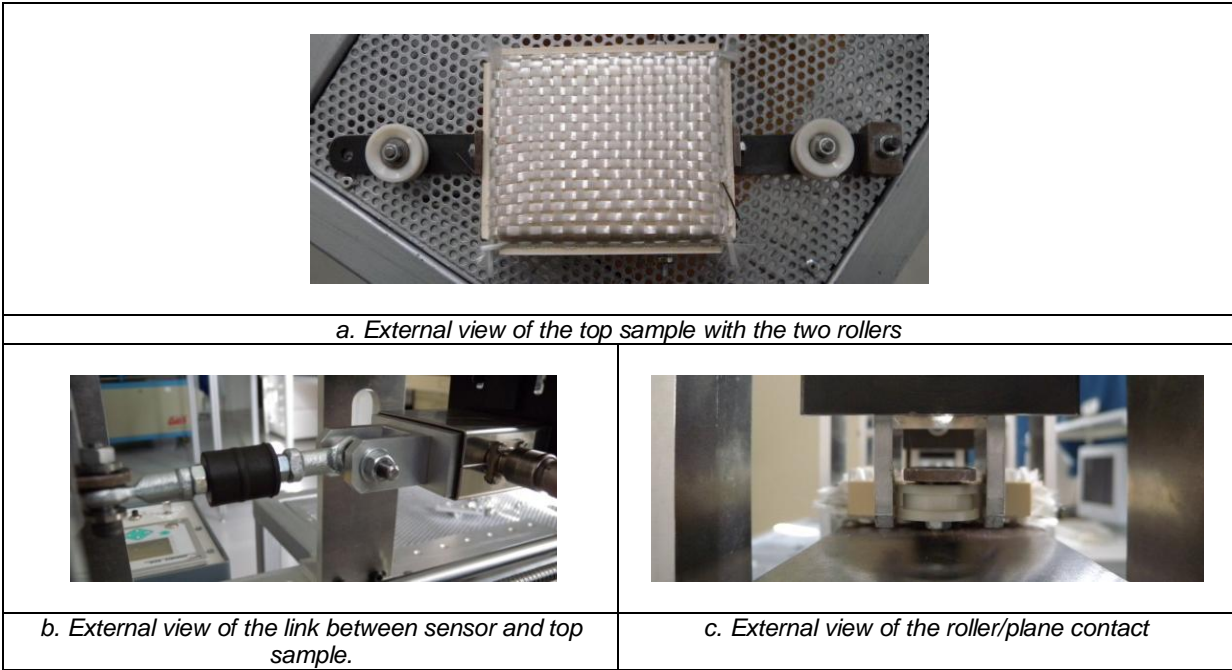


Figure 22 : external view of the top unit of the device

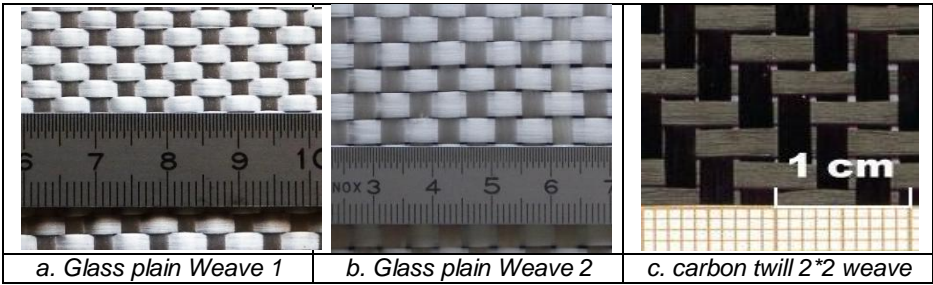


Figure 23 : fabrics used for fabric/fabric friction

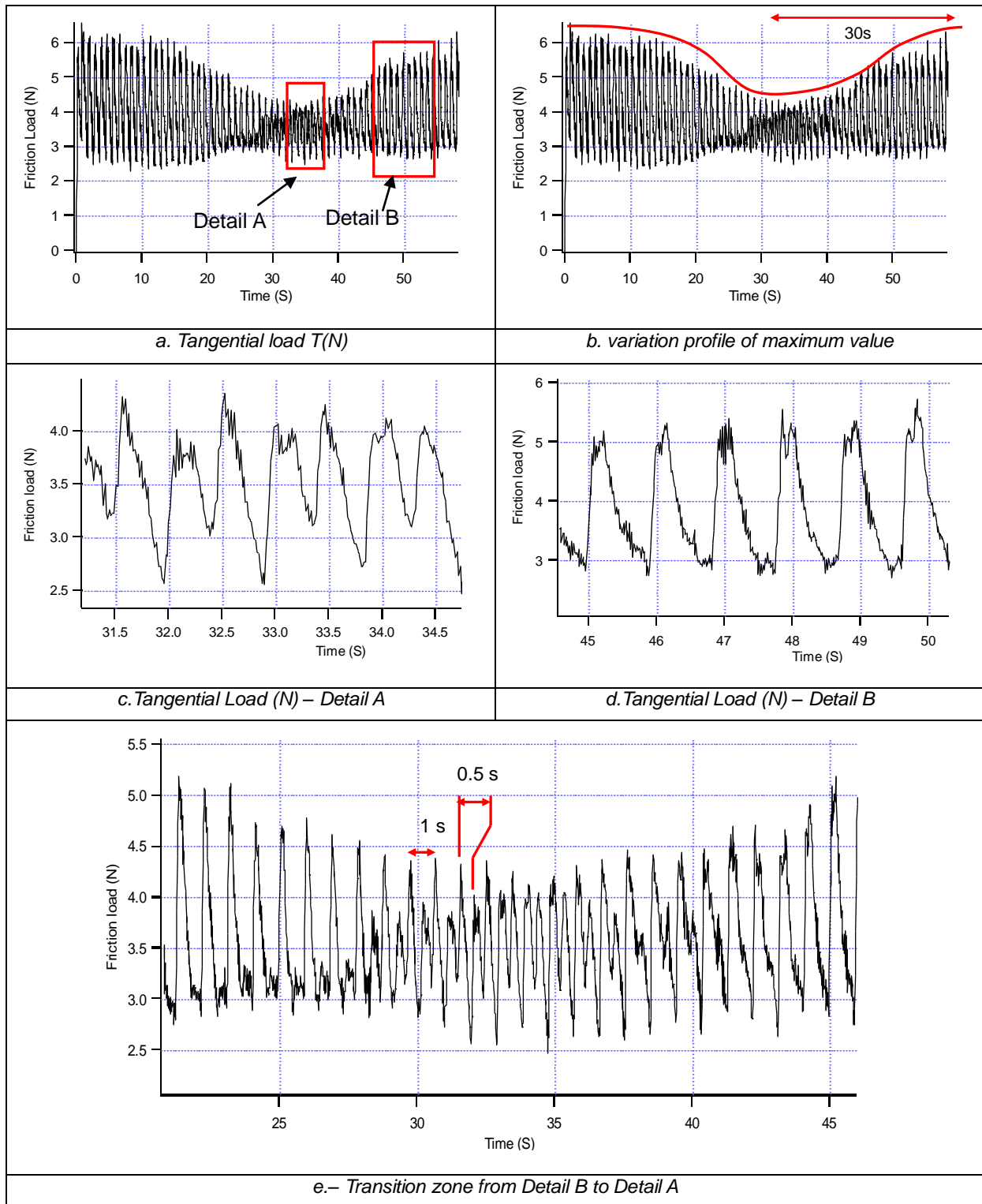


Figure 24 : Experimental results for the Glass plain weave 1, $v=5\text{mm/s}$, $N=10\text{N}$

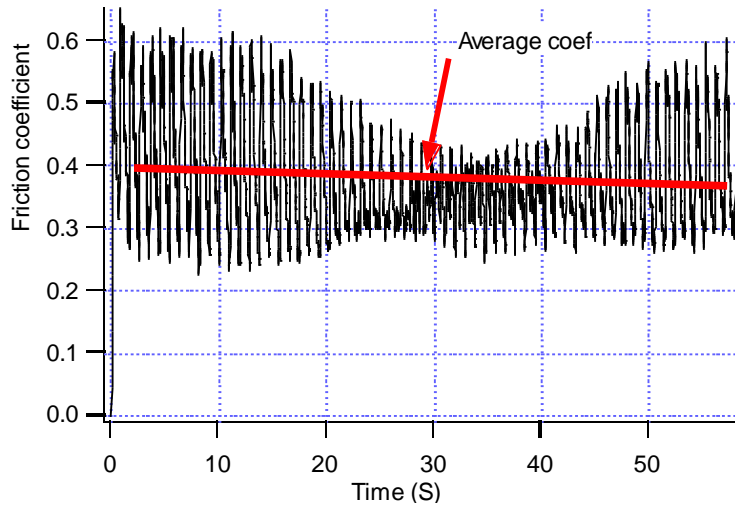


Figure 25 : Experimental time depending and average friction coefficient for the Glass plain weave 1, $v=5\text{mm/s}$, $N=10N$.

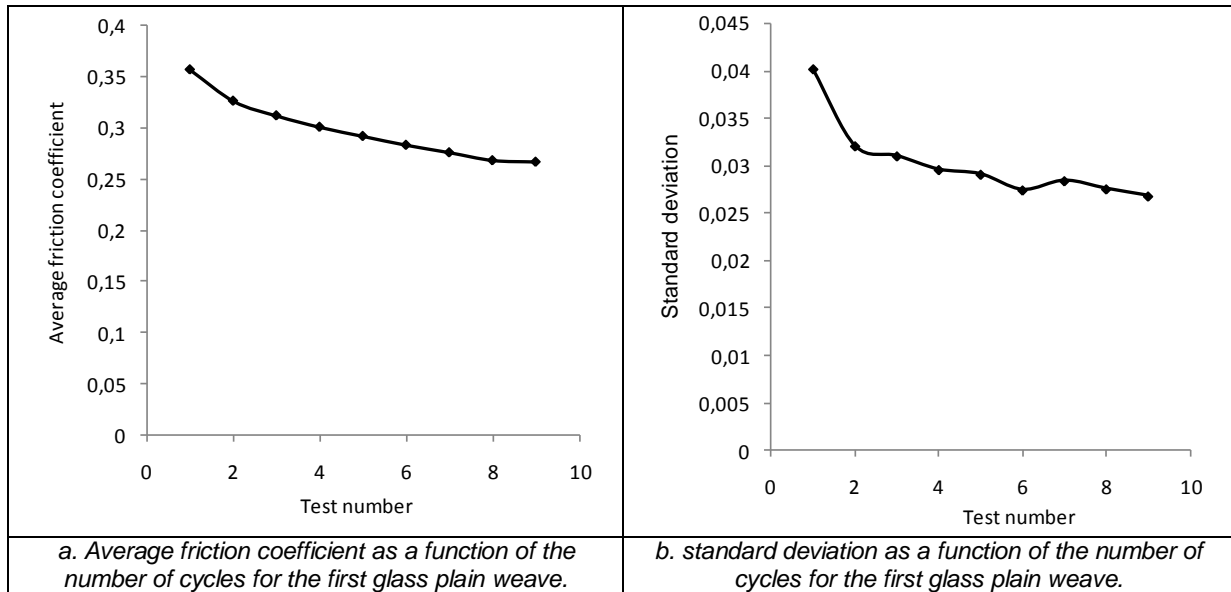


Figure 26 : average friction coefficient and standard deviation as a function of the number of cycles for a couple of the first glass plain weave samples, $v=5\text{mm/s}$, $N=10N$.

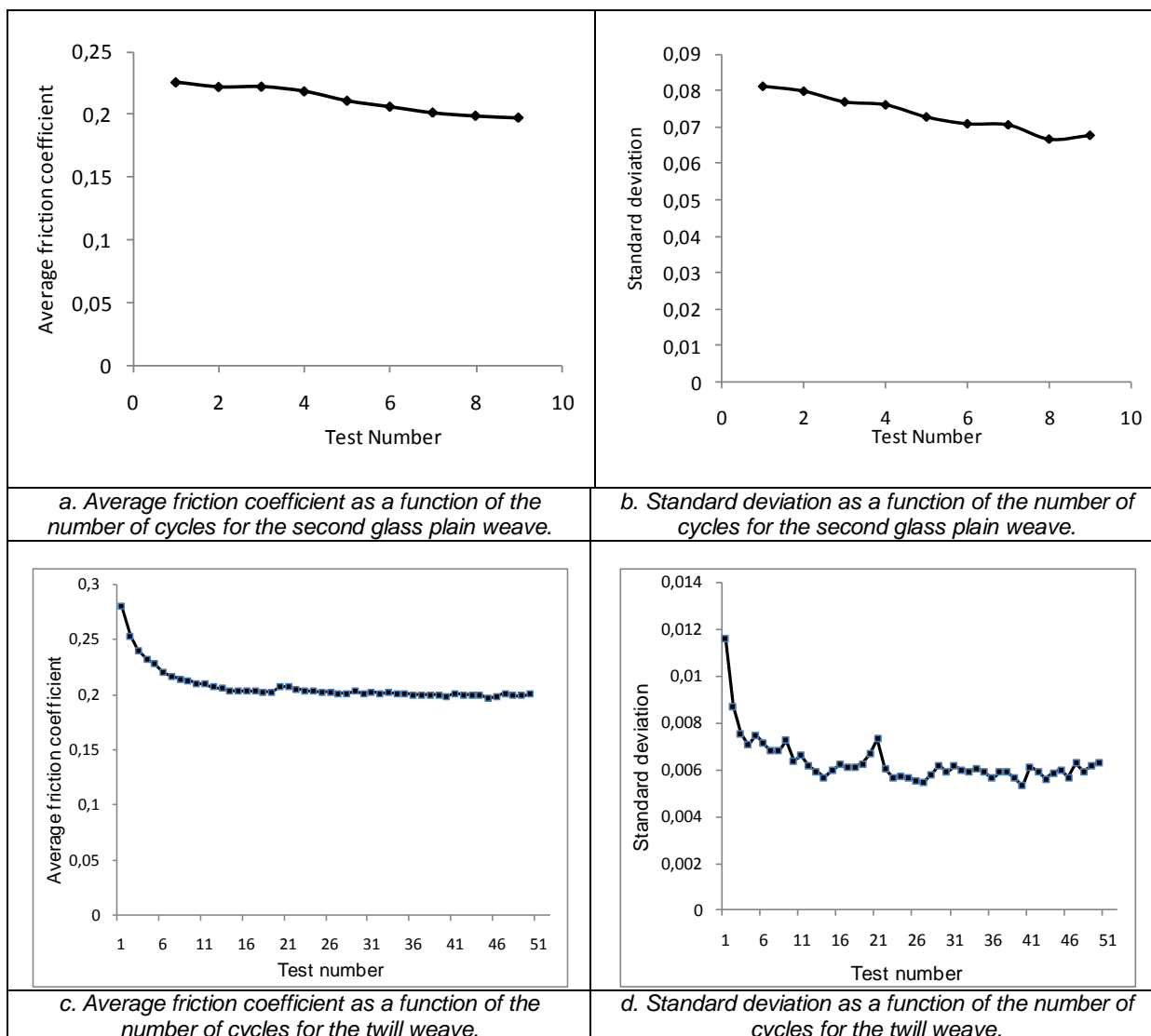


Figure 27 : Average friction coefficient as a function of the number of cycle for the 2nd glass plain weave (a., b.) and the carbon twill weave (c.,d.) .

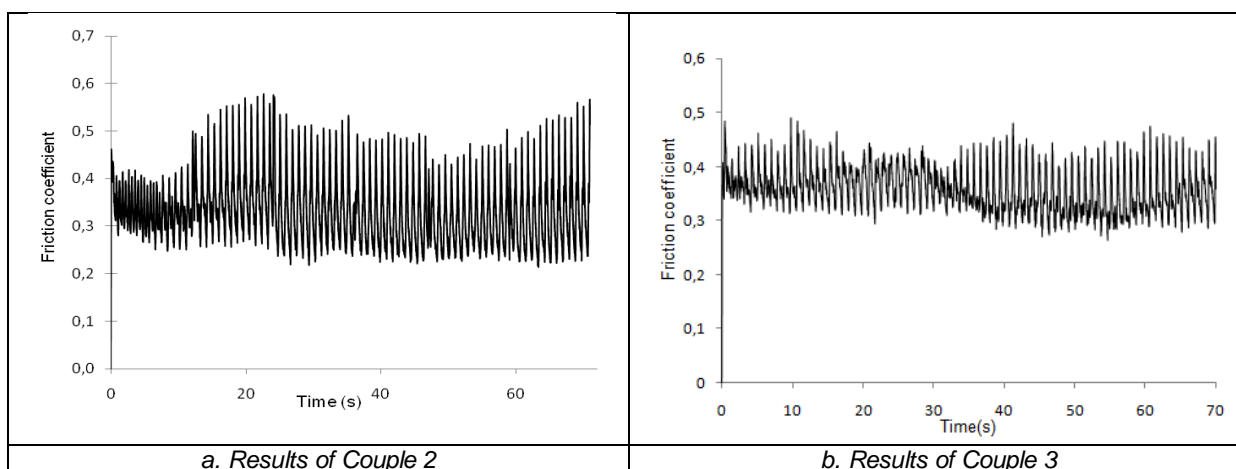


Figure 28 : friction coefficient results for 2 other identical samples of the glass plain weave 1.

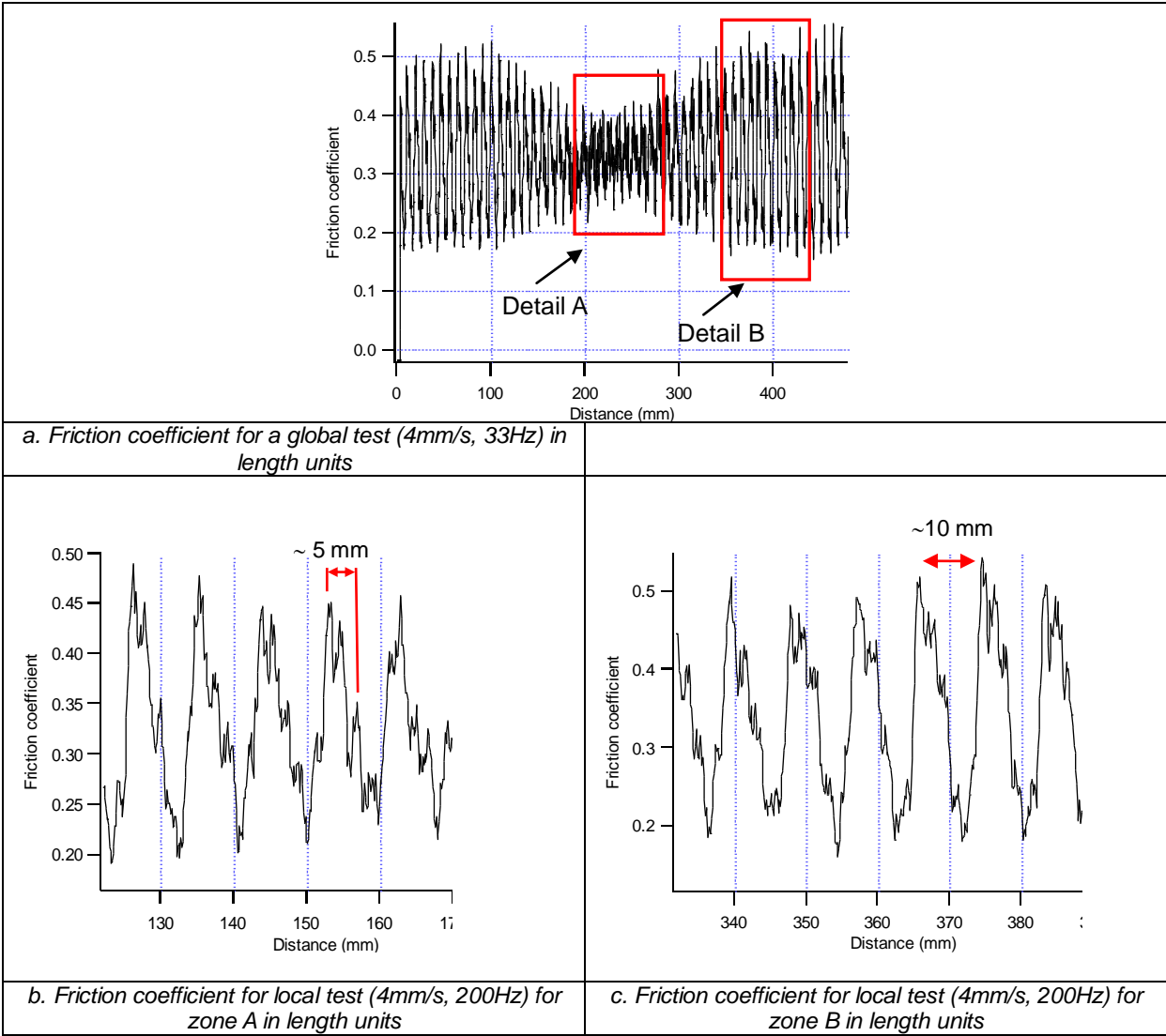
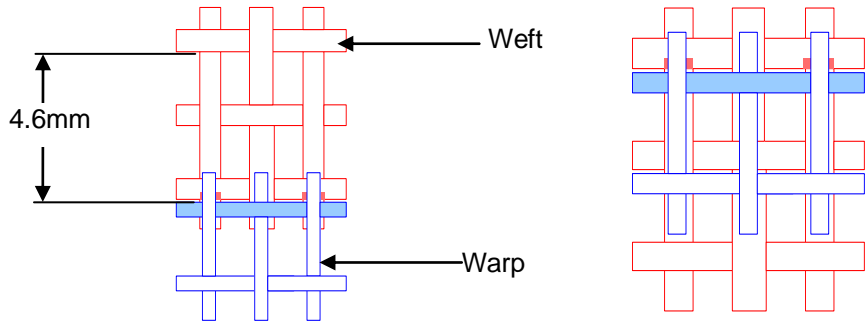
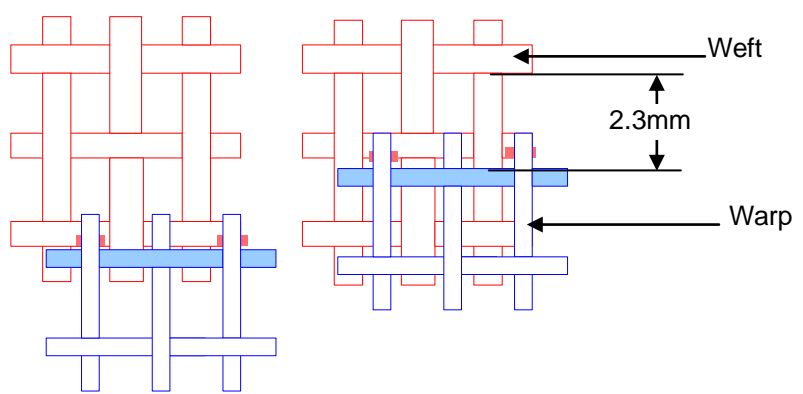


Figure 29 : Results for a couple of samples of the second glass plain weave, a. tangential force response, b, c. Periods in length units for zone A and B.



a. *Superimposed samples*



b. *Shifted samples*

Figure 30 Samples relative lateral positioning